BIOCHEMISTRY
including biophysical chemistry & molecular biology

Article

pubs.acs.org/biochemistry

The Slowdown of the Endoglucanase *Trichoderma reesei* Cel5A-Catalyzed Cellulose Hydrolysis Is Related to Its Initial Activity

Zhiyu Shu, Yefei Wang, Liaoyuan An, and Lishan Yao*

Laboratory of Biofuels, Qingdao Institute of Bioenergy and Bioprocess Technology, Chinese Academy of Sciences, Qingdao 266061, China

Supporting Information

ABSTRACT: One important feature of hydrolysis of cellulose by cellulases is that the reaction slows down quickly after it starts. In this work, we investigate the slowdown mechanism at the early stage of the reaction using endoglucanase *Tr.* Cel5A-catalyzed phosphate acid-swollen cellulose (PASC) hydrolysis as a model system. Specifically, we focus on the effect of enzyme adsorption on the reaction slowdown. Nineteen single mutations are introduced (with the assistance of molecular dynamics simulations) to perturb the enzyme PASC interaction, yielding the adsorption partitioning coefficient K_r that ranged from 0.12 to 0.39 L/g, compared to that of the wild type (0.26 L/g). Several residues, including T18, K26, Y26, H229, and T300, are demonstrated to be important for adsorption of the enzyme to PASC. The kinetic measurements show that the slowdown of the hydrolysis is not correlated with the adsorption quantified by the partitioning coefficient K_r but is anticorrelated with the initial activity. This result suggests that the mutants with higher activity are more prone to being trapped or deplete the most reactive substrate faster and the adsorption plays no apparent role in the reaction slowdown. The initial activity of Cel5A against PASC is correlated with the enzyme specific activity against a soluble substrate *p*-nitrophenyl cellobioside.

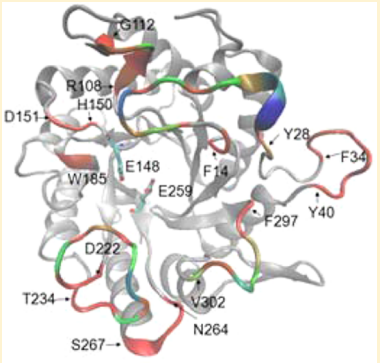

Cellulases can effectively hydrolyze cellulose, the most abundant renewable source of biomass on earth. Cellulases mainly include exoglucanases cleaving cellobiose from cellulose chain ends, endoglucanases cleaving chains randomly, and β-glucosidases converting cellodextrins to glucose. A prominent feature of the enzymatic hydrolysis of cellulose is the fact that the reaction rate declines as the reaction proceeds.[1,2] This slowdown has been attributed to product inhibition,[3,4] a decrease in substrate reactivity, e.g., depletion of easily hydrolyzed cellulose,[5,6] or the enzyme being trapped.[1] Pre-steady-state kinetic profiles of *Trichoderma reesei* exoglucanase and endoglucanases (including Cel7A,[7,8] Cel7B,[9,10] Cel5A,[11,12] and Cel12A[13])-catalyzed phosphate acid-swollen cellulose (PASC) hydrolysis show an initial burst of activity followed by a rapid decline.[14,15] This decline has been ascribed to the enzyme being trapped by the cellulose because the monitored reaction time is very short (<15 min) so that the product inhibition[16] or substrate reactivity decrease is very unlikely. Jalak et al. proposed an obstacle model to account for the slowdown of the hydrolysis by exoglucanases *Tr.* Cel7A and *Pc.* Cel7D.[17] After the cellulase is complexed with a cellulose chain, it cleaves the chain until reaching an obstacle that traps the enzyme. Though *Tr.* Cel5A, *Tr.* Cel7B, and *Tr.* Cel12A are endoglucanases, their processive hydrolysis ability is well-documented[18] and a similar trapping mechanism has been suggested.[14] The trapping of the enzyme results in a slow dissociation from the cellulose surface that hinders the enzyme recomplexation with a new cellulose chain and thus limits cellulose hydrolysis,[19] but the detailed mechanism of enzyme trapping especially at the molecular level is not clear. Is the trapping related to the enzyme binding? Furthermore, though the reaction time monitored in the pre-steady state is very short,[14,15] the substrate reactivity may still decrease because the substrate cellulose is insoluble and heterogeneous.

Tr. Cel5A is a key component of endoglucanases produced by *T. reesei*, and a lack of this enzyme reduces the endoglucanase activity by 55%.[20] The X-ray structure of the Cel5A catalytic domain (CD) adopts an $(\alpha/\beta)_8$ TIM-barrel fold.[11] *Tr.* Cel5A hydrolyzes the glycosidic bond through a retaining mechanism[21] with E148 as the general acid/base and E259 as the nucleophile. In this work, the *Tr.* Cel5A CD is selected as a model enzyme to investigate the trapping mechanism. A recent study of *Tr.* Cel7A-catalyzed cellulose hydrolysis[19] suggests that the effect of CBM on enzyme dissociation is very weak. Eliminating the CBM and the O-glycosylated linker makes possible the active *Tr.* Cel5A expression in *Escherichia coli*[11,22] and thus greatly simplifies the cloning and expression process.

In this work, we focus on the early stage (~10 min) of the PACS hydrolysis catalyzed by *Tr.* Cel5A. We first build a Cel5A cellulose complex model and identify the amino acids or fragments that are computationally important for the binding. Then mutations are designed experimentally to test the

Received: June 6, 2014
Revised: October 20, 2014
Published: November 25, 2014

computational predictions. The *Tr.* Cel5A wild-type (WT) and mutant binding affinities for PASC and their catalyzed hydrolysis are measured. Meanwhile, their catalytic ability against the soluble substrate is monitored using *p*-nitrophenyl cellobioside (PNPC). The results show that the slowdown of the endoglucanase is directly correlated with its catalytic ability. Specifically, the *Tr.* Cel5A mutants with higher activity are more likely to lose catalytic capability [a similar phenomenon is seen when using the more crystalline cellulose filter paper (FP) as the substrate]. However, there is no correlation between the extent of the reaction slowdown and the enzyme binding affinity. Though several mutants display an initial catalytic rate against PASC higher than that of the WT, their ability to release a reducing sugar on a long time scale is comparable to that of the WT. Meanwhile, the initial catalytic rates of *Tr.* Cel5A and its mutants against PASC are correlated with their specific activities against PNPC.

MATERIALS AND METHODS

MD Simulation. The apo form *T. reesei* Cel5A crystal structure [Protein Data Bank (PDB) entry 3QR3][11] was used as a starting model. The protonation states of ionizable residues were determined on the basis of a pK_a analysis using PROPKA3[23] where the residue was assigned as protonated (deprotonated) if the predicted pK_a was larger (equal or smaller) than 5.0. The cellulose slab was modeled on the basis of the cellulose Iβ crystal structure presented by Nishiyama et al.[24] The cellulose was three layers deep with five chains in each layer, and each chain includes 12 glucose units. Cel5A was docked on the cellulose surface manually using Hex,[25] so that the active site binding groove of Cel5A aligned with the middle cello-oligomer chain in the top layer (Figure S1 of the Supporting Information).

The simulations were conducted with Gromacs 4.5.[26,27] The gromos53a6[28,29] force field was employed to model the enzyme and the cellulose. The model was immersed in a dodecahedron box of explicit water molecules, with a 10.0 Å distance between the solvent box wall and the nearest solute atoms. In total, there were ∼31000 atoms for the apoenzyme and 60000 atoms for the enzyme cellulose complex system. The details of MD simulations are as follows. Initially, the systems were minimized for 1000 steps. Then, with all heavy atoms restrained by the harmonic potential (k = 239 kcal mol^{-1} nm^{-2}), the systems were equilibrated in a 100 ps *NVT* simulation. Finally, a 100 ns *NPT* MD simulation was performed for the apo and complex systems. In the complex simulation, the terminal glucose units of all cellulose chains were restrained with a force constant of 239 kcal mol^{-1} nm^{-2}. The MD snapshots were saved every 100 ps, and the first 60 ns simulations were treated as the equilibration period and thus not included in the data analysis. The hydrogen bond between Cel5A and cellulose was assigned when the distance of the two heavy atoms (O or N) is <3.5 Å and the angle (hydrogen−donor−acceptor) is <30°.

Cloning, Expression, and Purification. The DNA-encoding residues of the Cel5A CD from *T. reesei* QM9414 and a nine-His tag at the C-terminus were ligated with vector pET-22b, which was digested with the restriction enzymes NdeI and XhoI. The ligation mixture was transformed into *E. coli* strain DH10B. The correct coding sequence of the cloned catalytic domain of Cel5A gene was verified by DNA sequencing. The expression vector (pET-22b-Cel5A-CD) was then transformed into *E. coli* strain Rosetta-gami (DE3). All the mutations were made by polymerase chain reaction-based site-directed mutagenesis and verified by DNA sequencing. All the mutants were expressed and purified in a similar way. Briefly, 250 mL of LB medium containing 100 μg/mL ampicillin was inoculated with a fresh colony of expression strain Rosetta-gami (DE3) containing pET-22b-Cel5A-CD. The culture was grown at 37 °C while being vigorously shaken (∼200 rpm). When the OD_{600} of the culture reached 0.8−1.2, a final isopropyl β-D-1-thiogalactopyranoside concentration of 1 mM was added to induce the expression of the protein at 16 °C for 24 h. The cells were harvested by centrifugation, washed twice with water, resuspended in a 50 mM sodium phosphate buffer (pH 8.0), and lysed by ultrasonication. The lysed cells were centrifuged (9600*g* and 4 °C for 20 min), and the resulting supernatants were purified by Ni-NTA affinity chromatography (Novagen). The purity was determined by sodium dodecyl sulfate−polyacrylamide gel electrophoresis. The protein concentration was determined by measuring the UV absorption at 280 nm, with an extinction coefficient of 67880 M^{-1} cm^{-1}, calculated from the amino acid composition by using the online tool ProtParam (http://web.expasy.org/protparam/).

Adsorption Assays. All the assays were conducted in a 50 mM sodium acetate buffer at pH 5.0. PASC was prepared from Avicel powder using the method from the literature;[30] 200 μL mixtures containing 5 g/L PASC with Cel5A (WT or mutants, ranging from 0.4 to 1.4 μM) were incubated at 4 °C for 1 h. The free enzyme concentration was determined as follows. The incubated sample was centrifuged, and 20 μL of the supernatant was taken out and mixed with a 20 μL PNPC (final concentration of 2 mM) solution. The reaction was conducted at 50 °C for 120 min, and an aliquot of 35 μL was transferred to a microplate containing 165 μL of 1 M Na_2CO_3. The amount of product *p*-nitrophenol released was determined by measuring the sample absorbance at 405 nm using a microplate reader (Ultrospec visible plate reader II 96, GE Healthcare Bio-Science). A standard curve of the released *p*-nitrophenol was determined for each Cel5A. The enzyme concentration in the supernatant of the adsorption assay was back-calculated using the standard curve, from which the bound enzyme concentration was also obtained. One potential complication is that the released cellobiose during the incubation may inhibit Cel5A. This inhibition can cause an underestimation of the enzyme concentration in the supernatant. The maximal concentration of reducing sugar after incubation at 4 °C for 1 h is <1 mM (see Results and Discussion). To measure the inhibition effect of the product, 2.5 mM (final concentration) cellobiose was mixed with WT Cel5A (0.1, 0.2, and 0.35 μM), and it appeared that the enzyme concentration determined using the method described above was not affected by the presence of cellobiose (Figure S2 of the Supporting Information). All the adsorption assays were performed in duplicate.

Kinetic Assays. For the kinetic measurement with PNPC as the substrate, 40 μL mixtures containing 2 mM substrate and 4 μM Cel5A were incubated at 50 °C. The concentrations of the released *p*-nitrophenol, at time points of 0, 10, 20, 30, 40, and 50 min, were determined in the same way as described above. A linear fit was performed for the product concentration versus time to extract the enzyme specific activity (units per milligram) against PNPC, which is defined as the amount of reducing sugar (micromoles) released per minute per milligram of enzyme. For WT Cel5A, k_{cat} and K_m were also determined using the following experimental details. Forty microliters of mixtures of PNPC (1, 2, 3, 4, 5, 6, 7, and 8 mM) and WT

dx.doi.org/10.1021/bi501059n | *Biochemistry* 2014, 53, 7650−7658

Cel5A (4 μM) were incubated at 50 °C (PNPC has a solubility of ~8 mM at room temperature). The mixtures were reacted for 0, 10, 20, 30, 40, and 50 min, and 35 μL portions of reaction mixtures were taken out and added to 165 μL of 1 M Na_2CO_3 to stop the reaction. The amount of *p*-nitrophenol liberated was determined, and the reaction rate was extracted from the linear fitting of the product concentration versus time. The standard Michaelis–Menten equation was applied to fit the rates to obtain k_{cat} and K_m values using an in-house script.

For the kinetics of PASC hydrolysis, 200 μL mixtures containing 5 g/L PASC and 1 μM Cel5A were incubated for 1 h at 4 °C and then transferred to a 50 °C thermostat. For WT Cel5A, different enzyme concentrations of 0.1, 0.25, 0.5, and 2 μM were also used for the reaction. Amounts of reducing sugar, at time points of 0, 2, 4, 6, 8, and 10 min, were determined by the PHBAH method.[31] The reaction was stopped at different time points by filtering the reaction mixture through a 0.22 μm filter that effectively separated the supernatant from PASC. For the kinetics of FP hydrolysis, 200 μL mixtures containing 50 g/L FP and 1 μM Cel5A were incubated for 1 h at 4 °C and then transferred to a 50 °C thermostat. Amounts of reducing sugar were determined at time points of 0, 20, 40, 60, 80, 100, 120, 140, 160, and 180 min.

Processivity Measurements. Mixtures (200 μL) containing 5 g/L PASC and 1 μM Cel5A were incubated for 10 min at 50 °C. Reaction mixtures (25 μL) were taken out and used to determine the total reducing sugar concentration. The rest of the mixtures were then filtered through a 0.22 μm filter to remove all insoluble matter before the determination of the soluble reducing sugar concentration.

RESULTS AND DISCUSSION

Predicting Cel5A Binding Residues and Fragments. A model of *Tr.* Cel5A bound to an Iβ cellulose crystal was built and appeared to be stable in the 100 ns MD simulation run (Figure S3 of the Supporting Information), with the backbone C_α root-mean-square deviation (rmsd) from the X-ray crystallography structure (PDB entry 3QR3)[11] fluctuating around 0.2–0.3 nm, comparable to the value from the apo form Cel5A MD run. The C_α root-mean-square fluctuation (rmsf) from the average structure is also similar in the two simulations (Figure S4 of the Supporting Information), with the complexed enzyme displaying slightly higher rmsfs. Residues within 0.5 nm of the cellulose, identified in the simulation of the complex, are mapped on the three-dimensional structure (Figure 1) and colored according to the interaction energies between individual residues and the cellulose. The detailed interaction energies are also listed in Table S1 of the Supporting Information. Most contacting residues are located in the loop or short secondary structure regions (including residues 14–28, 34–40, 108–112, 150, 151, 185, 222–234, 264–267, and 297–302), which might be beneficial for catalysis because these regions are relatively flexible and thus can adopt different conformations to adsorb to cellulose. Among 20 residues having interaction energies of >1 kcal/mol, nine have hydrogen bonding interactions with the hydroxyl groups of the cellulose (Table S2 of the Supporting Information), highlighting the importance of electrostatics for the binding of the enzyme. Ten residues, including T18, D19, S25, K26, Y28, N38, N110, D224, H229, and T300, were selected for the experimental tests.

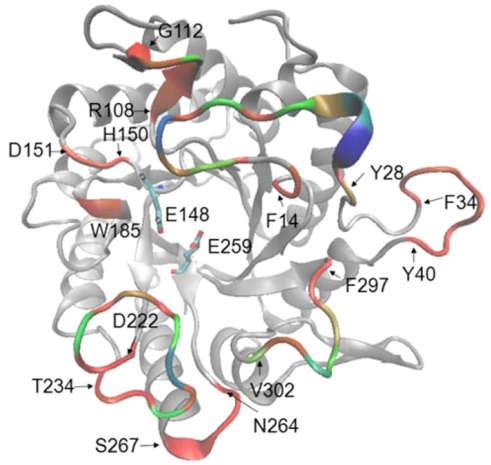

Figure 1. Interactions between Cel5A and the cellulose predicted by the MD simulation. Red, green, and blue colors correspond to the weak, medium, and strong interactions, respectively. The exact interaction energies are listed in Table S1 of the Supporting Information. The beginning and end of each fragment that has atoms within 5 Å of the cellulose are labeled, together with the catalytic acid E148 and the nucleophile E259.

Binding Affinities of the WT and Mutants for PASC. The adsorption of cellulase is commonly described by Langmuir isotherm

$$B = (B_{max}K_aF)/(1 + K_aF) \quad (1)$$

where B is the bound enzyme concentration, F is the free enzyme concentration, and K_a is the association constant. In the linear region of the Langmuir curve where K_aF is much smaller than 1, eq 1 can be simplified

$$B = K_rF \quad (2)$$

where K_r is a relative association constant or partitioning coefficient, defined as $B_{max}K_a$.[32] The parameter K_r can be determined by the linear fitting of the bound form versus the free form enzyme using eq 2. For WT Cel5A adsorption, a linear correlation was observed as expected, but using eq 2 did not yield a satisfactory fit. Adding a second parameter (using $B = K_rF + c$) improved the fitting, and a positive intercept c was obtained (Figure 2), indicating the existence of the high-affinity (but low-capacity) binding of Cel5A to PASC. The K_r of adsorption of WT Cel5A to PASC is 0.26 ± 0.01 L/g, with an

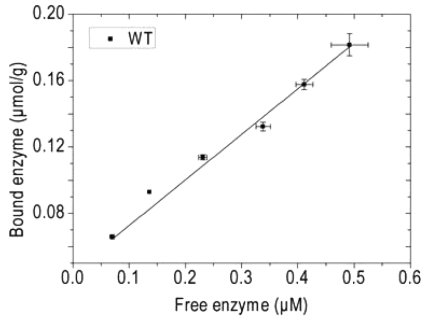

Figure 2. Adsorption of WT Cel5A to PASC. The total protein concentration range was 0.4–1.4 μM, and the substrate concentration was 5 g/L. The best-fit line is $y = 0.26x + 0.052$, with a Pearson correlation coefficient (R_p) of 0.99.

dx.doi.org/10.1021/bi501059n | *Biochemistry* 2014, 53, 7650–7658

Table 1. Adsorption Affinities of Cel5A and Its Mutants for PASC and Corresponding Kinetic Parameters with PASC or PNPC as the Substrate

enzyme	K_r (L/g)	c ($\times 10^{-1}$ μmol/g)	A (mM/min)	b	specific activity[a] ($\times 10^{-3}$ units/mg)
WT	0.26 ± 0.01	0.52 ± 0.04	0.31 ± 0.04	0.76 ± 0.07	6.14 ± 0.19
T18A	0.21 ± 0.01	0.73 ± 0.03	0.52 ± 0.05	0.54 ± 0.05	6.86 ± 0.15
T18D	0.12 ± 0.01	0.26 ± 0.06	0.29 ± 0.02	0.66 ± 0.03	4.43 ± 0.09
D19A	0.25 ± 0.02	0.54 ± 0.06	0.16 ± 0.01	0.88 ± 0.03	4.37 ± 0.10
D19Y	0.16 ± 0.01	0.68 ± 0.05	0.21 ± 0.01	0.88 ± 0.02	4.66 ± 0.13
S25D	0.38 ± 0.02	0.76 ± 0.07	0.27 ± 0.02	0.81 ± 0.03	4.30 ± 0.11
S25Y	0.39 ± 0.03	0.79 ± 0.06	0.47 ± 0.03	0.61 ± 0.06	5.98 ± 0.16
K26A	0.20 ± 0.02	0.59 ± 0.08	0.28 ± 0.02	0.81 ± 0.03	6.06 ± 0.23
Y28A	0.17 ± 0.01	0.50 ± 0.03	0.23 ± 0.02	0.83 ± 0.04	3.54 ± 0.08
Y28W	0.24 ± 0.02	0.81 ± 0.07	0.36 ± 0.02	0.63 ± 0.03	5.34 ± 0.15
N38A	0.24 ± 0.02	0.56 ± 0.07	0.42 ± 0.04	0.62 ± 0.05	5.92 ± 0.20
N38D	0.23 ± 0.01	0.57 ± 0.04	0.37 ± 0.03	0.67 ± 0.04	6.17 ± 0.27
N39D	0.24 ± 0.02	0.84 ± 0.04	0.39 ± 0.02	0.66 ± 0.02	6.21 ± 0.23
Y40F	0.26 ± 0.03	0.75 ± 0.07	0.35 ± 0.05	0.68 ± 0.07	6.27 ± 0.26
N110A	0.26 ± 0.02	0.87 ± 0.06	0.30 ± 0.01	0.68 ± 0.01	5.17 ± 0.18
N110D	0.23 ± 0.04	0.83 ± 0.10	0.23 ± 0.02	0.82 ± 0.05	5.63 ± 0.21
D224A	0.24 ± 0.04	0.72 ± 0.10	0.20 ± 0.01	0.71 ± 0.03	3.53 ± 0.03
H229A	0.17 ± 0.01	0.73 ± 0.05	0.33 ± 0.01	0.62 ± 0.02	4.57 ± 0.10
T300A	0.20 ± 0.02	0.83 ± 0.06	0.46 ± 0.06	0.61 ± 0.06	6.07 ± 0.23
T300Y	0.33 ± 0.04	0.68 ± 0.09	0.49 ± 0.06	0.57 ± 0.06	6.35 ± 0.29

[a]The specific activity was determined for PNPC.

intercept of 0.052 ± 0.004 μmol/g (Table 1). To test whether the positive intercept is due to high-affinity binding, we measured the WT enzyme activity at the low enzyme concentration of 0.25 μM, which is smaller than c multiplied by the substrate PASC concentration (0.052 μmol/g × 5 mg/mL = 0.26 μM). In other words, the enzyme should be all adsorbed. The kinetic data show that it has a rather high activity (Figure S5 of the Supporting Information; see the discussion below), suggesting that the intercept is due to the high-affinity but low-capacity binding. It would be interesting to know whether this high-affinity binding is reversible, but the concentration of free enzyme on the supernatant is lower than the detection limit (~0.05 μM) and thus cannot be measured accurately.

Nine residues interacting with the cellulose predicted by the MD simulation were mutated to alanine (one at a time), and their adsorption affinities were measured. Four alanine mutations, T18A, D19A, K26A, and Y28A, from the fragment of residues 14−28 show weakened binding. Among these four mutants, Y28A has the lowest binding affinity. As predicted by the MD simulation, the main interaction between residue Y28 and the cellulose is from the van der Waals contribution, suggesting that the tyrosine ring stacks with the glucose unit of cellulose. This is consistent with mutant Y28W binding where the tryptophan ring regains the interaction with the cellulose, yielding a partitioning coefficient (0.24 ± 0.02 L/g) close to that of the WT. T18A has a K_r of 0.21 ± 0.01 L/g, ~20% smaller than that of the WT, and the T18D mutation further decreases K_r to 0.12 ± 0.01 L/g. Similarly, D19A has a K_r of 0.25 ± 0.02 L/g and D19Y a lower K_r of 0.16 ± 0.01 L/g. But for residue K26 that is predicted by MD to have the strongest interaction [−19.5 kcal/mol (Table S1 of the Supporting Information)] with cellulose through the side chain amino group, the mutation to alanine decreases the K_r by only 20% compared to that of the WT. It is likely that the cellulose−lysine interaction is offset by the penalty of solvation energy of the positive charge when the enzyme adsorbs to cellulose so that the net binding contribution from K26 is small. On the other hand, mutants S25D and S25Y both increase the K_r by ~50%. The experimental data overall confirm the importance of residues in the fragment of residues 14−28 to Cel5A adsorption.

The MD simulation shows that the fragment of residues 34−40 is also in contact with the cellulose, but the interaction between the two is relatively weak [<1 kcal/mol for residue specific interaction energies (Table S1 of the Supporting Information)]. Four mutations, N38A, N38D, N39D, and Y40F, from the fragment of residues 34−40 are introduced, and all show a binding affinity equal to or weakened compared to that of the WT, but the difference in K_r is quite small, consistent with the MD prediction. In the fragment of residues 108−112, N110 has the largest energy of interaction with cellulose [−3.5 kcal/mol (Table S1 of the Supporting Information)]; however, N110A has the same binding affinity as the WT, and N110D deceases K_r by only ~10%. In the fragment of residues 222−234, H229 is predicted to interact most strongly with cellulose (−12.8 kcal/mol). Mutant H229A has a K_r that is 35% smaller than that of the WT. But for another residue D224, which has an energy of interaction with the cellulose of −6.3 kcal/mol, the mutation to alanine has no effect on the binding constant K_r. Another important binding residue tested by the experiment is T300; mutant T300A decreases K_r by 23%, and mutant T300Y increases K_r by 27%. It is worth noting that mutations not only change the partitioning coefficient K_r but also alter the high-affinity binding parameter c. For example, T18D has the smallest c and K_r. A weak positive correlation is obtained between c and K_r (Figure S6 of the Supporting Information), suggesting that high-affinity binding is also affected by the binding residues and the two binding modes are somehow related. Discrepancy occurs between the experimental adsorption and computational predictions. The main reason is that the binding energies decomposed from the MD simulation are not free energies and thus cannot be compared quantitatively with K_r, but qualitatively, one can

dx.doi.org/10.1021/bi501059n | Biochemistry 2014, 53, 7650−7658

argue that the residues with more negative binding energies tend to be more important for the interactions between the enzyme and cellulose. Thus, the MD simulation provides important information for identifying the potentially important binding residues. Though not all the binding residues predicted by the MD simulation are tested experimentally, the variation of K_r among the WT and 19 mutants (0.12−0.39 L/g) is sufficiently large for investigating the relationship between binding and enzyme catalysis.

Kinetics of the WT and Mutants. Kostylev et al. used a power function to describe the cellulose hydrolysis catalyzed by cellulases[33,34]

$$P_{tot} = At^b \quad (3)$$

where P_{tot} is the total product concentration, A is the activity of the enzyme, b is the hydrolysis power factor that is generally <1, and t is the time. A is the product of the specific activity and the concentration of the bound active enzyme. The parameter b describes the curvature of the fitting curve, and a higher b value implies the enzyme is more effective at overcoming the recalcitrance of cellulose[34] and thus less likely to be trapped by the substrate. The plot of P_{tot} versus time is shown in Figure 3

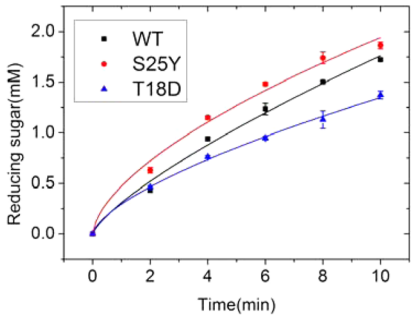

Figure 3. Fitted hydrolysis curves for Cel5A and mutants T18D and S25Y. The reaction mixture contains 1 μM enzyme and 5 g/L PASC [50 mM NaAc (pH 5.0)]. The three best-fit curves are $y = 0.31x^{0.76}$ (WT), $y = 0.29x^{0.66}$ (T18D), and $y = 0.47x^{0.61}$ (S25Y). The sugar concentration at time zero was treated as the background and subtracted out so that the curves go through the origin.

for WT Cel5A and mutants T18D and S25Y. As one can see, the model fits quite well to the experimental data. For the WT, A is equal to 0.31 ± 0.04 mM/min and b is 0.76 ± 0.07. Compared to the classical enzyme kinetics that has a b value of 1, the effect of the b value of 0.76 in slowing the reaction is quite substantial. For example, after reaction for 10 min, the total product concentration will be 0.31 × 10 = 3.1 mM if b = 1 and $0.31 \times 10^{0.76}$ = 1.8 mM if b = 0.76.

The kinetic parameters for the WT and all the mutants are listed in Table 1. For the fragment of residues 14−28, which is involved in enzyme binding, the nine mutants show a large variation of A (0.16−0.52 mM/min) and b (0.54−0.88). Among these mutants, T18A has the highest A value of 0.52 ± 0.05 mM/min, ∼68% larger than that of the WT. T18A also shows an activity against PNPC higher than that of the WT, though with a much smaller difference, only ∼10%. T18 is near E148, with the shortest distance between C_γ of T18 and O_ε of E148 being 6.0 Å. This mutation may perturb the conformation of E148 to impact the enzyme activity, but the small difference in activity against PNPC indicates this perturbation should be small. The adsorption constant K_r of T18A is ∼20% smaller than that of the WT, so the amount of bound enzyme is smaller for the mutant, suggesting that T18A is more effective in hydrolyzing PASC. However, the bound active enzyme concentration, which is difficult to measure, may be different from that determined in the adsorption assay. Though T18A has the largest A, it also has the smallest b value of 0.54 ± 0.05, indicating that this mutant is more prone to being slowed by PASC. As a result, the amount of product released by the mutant at the longest measurement time point (10 min) is comparable to that of the WT (Table S3 of the Supporting Information). Compared to T18A, the mutation to aspartate at the same site yields a much smaller A (0.29 ± 0.02 mM/min). T18D also has a smaller partitioning coefficient to PASC (K_r = 0.12 ± 0.01 L/g), only ∼50% of that of the WT or T18A, but has a b value (0.66 ± 0.03) between those of the WT (0.76 ± 0.07) and T18A (0.54 ± 0.05), demonstrating that K_r is not correlated to b for this residue. D19A has the smallest A (0.16 ± 0.01 mM/min) and the largest b of 0.88 ± 0.03 at the same time. The small A of D19A is in concert with its low PNPC activity, which is ∼30% lower than that of the WT (Table 1). Besides D19A, several other mutants from this fragment, including T18D, D19Y, S25Y, and Y28W, display a PNPC activity 13−30% lower than that of the WT, suggesting that the mutations at these sites perturb the active site structure. Though the variations of b (0.54−0.88) and K_r (0.12−0.39) are quite substantial for the mutations in the fragment of residues 14−28, there is no direct correlation between the two measurables. A lack of correlation between K_r and b suggests that the binding change in this region does not play a major role in the enzyme's activity decrease in hydrolyzing PASC.

Four mutants, N38A, N38D, N39D, and Y40F, from the fragment of residues 34−40 all show A values (10−35%) larger than as well as b values (10−20%) slightly smaller than those of the WT. Their activities against PNPC are comparable to that of the WT, which is not surprising because they are approximately ≥25 Å from the catalytic acid E148 and the nucleophile E259 (Figure 1). N110A has an A value comparable to that of the WT but a smaller b, whereas N110D has a smaller A but a larger b. Both mutants slightly decrease the PNPC activity, though N110 is ∼16 Å from E148 and 18 Å from E259. D224 forms a salt bridge with H226, as suggested by the X-ray structure.[35] Mutants D224A and H226A decrease the enzyme's specific activity against PNPC and have b values smaller than that of the WT, though both residues D224 and H226 are away from the active sites, with a distance of ∼12 Å between D224 and E148 and ∼14 Å between H226 and E259. T300A and T300Y increase A by 48 and 58% but decease b by 20 and 25%, respectively, and both mutants have a PNPC specific activity similar to that of the WT (Table 1). On the other hand, the amounts of reducing sugar released after PASC hydrolysis catalyzed by the two mutants for 10 min are also comparable to that of the WT (Table S3 of the Supporting Information).

Fitting of the Kinetic Parameters Using a Different Model. One limitation of the power equation (eq 3) is that the first-order derivative at time zero, corresponding to the initial reaction rate, is infinity provided that b is <1. An empirical formula was developed by Ohmine et al.[36] to describe the time evolution of the product concentration:

$$P_{tot} = \frac{S_0}{k} \ln(1 + v_0 kt/S_0) \quad (4)$$

where S_0 is the initial substrate concentration, v_0 is the reaction rate at time zero, and k is the retardation constant. Fitting of

dx.doi.org/10.1021/bi501059n | Biochemistry 2014, 53, 7650−7658

the Cel5A PASC hydrolysis data to eq 4 yields v_0 and k (Table S4 of the Supporting Information). A positive linear correlation is observed between A and v_0 (Figure S7A of the Supporting Information), suggesting that A is related to the initial reaction rate. A negative correlation is shown between b and k (Figure S7B of the Supporting Information), so that the enzyme with a larger k is more likely to be slowed. Though the two kinetic models have quite different formulas, they produce consistent kinetic parameters.

Kinetics versus Binding. An early work by Nidetzky[37] showed that it takes ~40 min to reach the binding equilibrium for the adsorption of the Cel5A CD to FP. The longest reaction time is 10 min in this work, which is rather short to avoid the product inhibition and potential substrate reactivity change (see the discussion below).[14] Therefore, one cannot simultaneously measure the kinetics and binding constant because the binding is not in equilibrium (which can complicate the interpretation of kinetic data). Extra incubation time (1 h at 4 °C) was introduced to allow the Cel5A PASC binding to reach equilibrium before the reaction starts at 50 °C. The concentration of reducing sugar released during incubation, ranging from 0.32 to 0.90 mM (Table S3 of the Supporting Information), was subtracted out in the kinetic data fitting. One complication of this experimental setup is that the faster reaction rate measured at 50 °C may be related to the quicker release of the enzyme that was bound at 4 °C. To test this, the free enzyme concentration in the supernatant was monitored during the reaction at 50 °C, for two mutants T18A and D19A that have the largest activity differences [~3-fold (Table 1)]. The amount of free enzyme for both mutants shows a slight increase from 0.3 μM at time zero to 0.35 μM at 10 min (Figure S8 of the Supporting Information), likely caused by the small binding affinity difference at 4 and 50 °C. Apparently, the 3-fold difference in activity A between D19A and T18A is not due to the release of the enzyme from PASC that occurs for both mutants. A positive correlation is observed between activity A and the specific activity against PNPC for Cel5A and the mutants (Figure 4), suggesting that the parameter A is related to the activity of the enzyme in hydrolyzing soluble substrate. For WT Cel5A, the Michaelis–Menten kinetics with PNPC as the substrate was studied, yielding a k_{cat} of 3.0 ± 0.6 min^{-1} and a K_m of 40 ± 9 mM (Figure S9 of the Supporting Information). This K_m value is considerably larger than 2 mM, the PNPC concentration used for the specific activity assay for the WT and mutants. Apparently, the measured PNPC specific activity reflects k_{cat}/K_m rather than k_{cat} alone. The correlation between b and K_r is poor (Figure S10 of the Supporting Information), suggesting that the slowdown of Cel5A-catalyzed PASC hydrolysis is not related to the enzyme adsorption, which is prerequisite for catalysis. Meanwhile, the correlation between b and c is also poor (Figure S10B of the Supporting Information), suggesting that the high-affinity binding plays no role in the reaction slowdown.

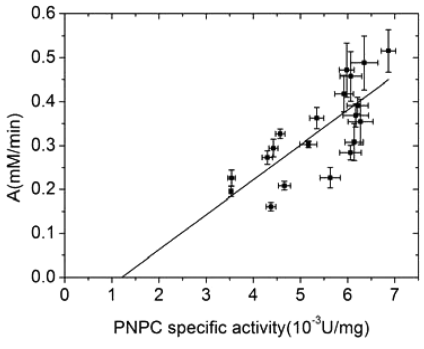

Figure 4. Correlation between the Cel5A activity A against PASC and its specific activity against PNPC. The PNPC hydrolysis reaction mixture contains 4 μM enzyme and 2 mM PNPC [50 mM NaAc (pH 5.0)]. The best-fit line is $y = 79x - 0.10$, with a correlation coefficient (R_p) of 0.76. The positive correlation suggests that the activity parameter A is correlated with the enzyme's ability to hydrolyze the soluble substrate.

In this work, all the kinetics and binding data are only for the CD of Cel5A. It is known that the CBM is important for enzyme binding. Presumably, the mutational effect on binding affinity of full length Cel5A will be smaller than that of the Cel5A CD, but the activity against PASC is very likely correlated with that against PNPC. Therefore, we speculate that the correlation between the binding affinity and the activity for the full length Cel5A should be poor, as well.

Mechanism of the Slowdown of the Reaction. Like previous cellulose hydrolysis studies,[14,15,17,19] the rapid retardation is quite obvious for endoglucanase Cel5A. A trapping model was proposed for the slowdown of the hydrolysis by exoglucanases *Tr.* Cel7A and *Pc.* Cel7D[17] as well as endoglucanases *Tr.* Cel5A, *Tr.* Cel7B, and *Tr.* Cel12A.[14] The trapping is caused by an obstacle in the substrate cellulose. For amorphous cellulose PASC, the obstacle may come from the intertwined cellulose chains. Our results show that the extent of trapping, described by the hydrolysis power factor b, is negatively correlated with the catalytic rate A (Figure 5). This observation suggests that it is the length of the obstacle free path limiting the hydrolysis and the more active Cel5As simply reaches the end of the free path faster. It is surprising that 10 of the 19 mutants have A values larger than that of the WT, but very few mutants have a reducing sugar yield higher than that of the WT after reaction for 10 min. On the other hand, one would expect the trapping to shift the equilibrium to favor the bound state, which is seemly incompatible with the small increase in enzyme concentration during the PASC hydrolysis for T18A and D19A. Considering that the free enzyme concentration is lower than that of the bound form (0.6–0.7 μM) and it takes ~40 min to reach the binding equilibrium, the trapping of one portion of the bound enzyme may not be reflected immediately by the change in free enzyme concentration.

It has also been suggested by Hong[6] and Zhang[5] that a decrease in substrate reactivity is responsible for the slowdown of the reaction rate. In this work, the reaction time (maximum of 10 min) is much shorter than that in Hong and Zhang's studies but comparable to that in Murphy's study.[14] Murphy has shown through ITC experiments that the substrate PASC reactivity remains unchanged after, e.g., hydrolysis by *Tr.* Cel7B for 15 min.[14] To test the possibility of the decrease in reactivity, we used a much lower WT Cel5A enzyme concentration of 0.25 μM for the PASC hydrolysis, which yielded values of 0.15 ± 0.01 for A and 0.88 ± 0.05 for b (Figure S5 and Table S5 of the Supporting Information). This parameter A is approximately half of the value obtained at a WT enzyme concentration of 1 μM. Because A reflects the initial reaction rate, the enzyme at the low concentration appears to be more active if A is divided by the enzyme concentration. Furthermore, at the low enzyme concentration (0.25 μM), the b value of 0.88 ± 0.05 is also larger than that of 0.76 ± 0.07

dx.doi.org/10.1021/bi501059n | *Biochemistry* 2014, 53, 7650–7658

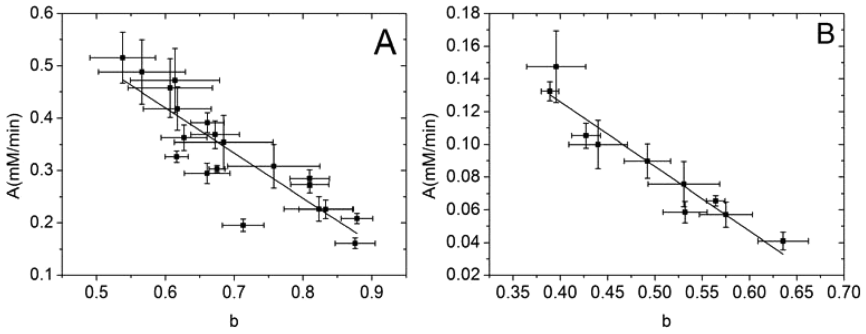

Figure 5. Correlation between the kinetic parameter A and b with PASC (A) or FP (B) as the substrate. Panel A includes parameters for WT Cel5A and 19 mutants (Table 1), whereas Panel B includes parameters for WT Cel5A and nine mutants (Table S5 of the Supporting Information). The best-fit lines are $A = -0.86b + 0.94$ and $A = -0.40b + 0.28$, with correlation coefficients (R_p) of −0.87 and −0.95 for panels A and B, respectively. The anticorrelation between the two parameters suggests that the slowdown of Cel5A catalysis is directly related to its activity.

at the high enzyme concentration (1 μM), suggesting that at the low enzyme concentration, the slowdown of the reaction is less obvious. This observation indicates that the decrease in substrate reactivity still plays some role. At a low enzyme concentration, the depletion of the most reactive sites is slower, so that the enzyme displays a relatively higher activity and a weaker tendency to be slowed. It was observed that the b value remains unchanged in the bacterial cellulose hydrolysis when the enzyme [*Thermobifida fusca* (*Tf.*) Cel48A and *Tf.* Cel5A] concentration is varied.[33] In this work, the b value seemingly decreases with an increase in enzyme concentration. To confirm this, a larger range of Cel5A concentrations (0.1−2 μM) was tested, and the same trend was observed (Table S5 of the Supporting Information). For example, the b value is 0.90 ± 0.02 at 0.1 μM enzyme and decreases to 0.69 ± 0.04 at 2 μM enzyme.

The third possible mechanism for the reaction slowdown is the inhibition of the product. The maximal concentration of reducing sugar released is <3 mM for the reactions monitored at 50 °C (Table S3 of the Supporting Information), which is much smaller than the IC_{50} of *Tr.* Cel5A,[16] so product inhibition is not responsible for the slowdown of catalysis.

In summary, the negative correlation between A and b is likely due to the trapping of the enzyme and the decrease in substrate reactivity. To test whether the negative correlation holds for a more crystalline substrate, we took the kinetic measurements using FP as the substrate for Cel5A and nine mutants that have large spans of A and b values for PASC (Table 1). For FP, it takes much longer to see the slowdown effect likely because of its recalcitrance to enzyme hydrolysis. The kinetic data for the FP substrate were fit quite well using eq 3 (Figure S11 and Table S6 of the Supporting Information). A strong negative correlation is seen between A and b, similar to that in PASC hydrolysis (Figure 5B).

It has been shown for chitinases that processivity is important for their catalytic efficiency. Specifically, chitinases with high processivity are more effective in hydrolyzing crystalline chitin but less effective in hydrolyzing chitosan, a soluble chitin derivative, than the mutants with reduced processivity.[38−41] For the hydrolysis of PASC by exoglucanase *Tf.* Cel48A, the lower-processivity mutants tend to have higher activity.[34] To test whether a similar effect occurs in Cel5A PASC hydrolysis, we determined the apparent processivity of Cel5A by using the ratio of the produced soluble reducing sugar concentration to the total reducing end concentration after reaction for 10 min. The apparent processivity has an average of 0.81 ± 0.02 over all the mutants and the WT (Table S7 of the Supporting Information). The variation is smaller than the average error of 0.06 propagated from the measurement. Thus, the effect of the mutation on the enzyme processivity is rather small, suggesting that the processivity is not responsible for the Cel5A activity differences.

Implications for Cellulose Degradation. Our work shows that for endoglucanase *Tr.* Cel5A, the slowdown of PASC hydrolysis cannot be alleviated by introducing the mutation with a lower binding affinity. Kostylev and Wilson demonstrated that the addition of *Tf.* E7,[33] an AA10 auxiliary enzyme capable of cleaving cellulose chains randomly through an oxidoreductive mechanism,[42,43] increases A and b simultaneously for *Tf.* Cel48A (an exoglucanase)-catalyzed bacterial cellulose hydrolysis. The random cleavage of cellulose chains by *Tf.* E7 creates more chain ends and reduces chain lengths, which partially removes the obstacles and enhances the substrate reactivity and thus the hydrolysis efficiency. It will be interesting to see whether this type of auxiliary enzyme is capable of significantly increasing the b values of those *Tr.* Cel5A mutants with high initial activities. Addition of xylanase[44,45] or mannanase[46] improves cellulase-catalyzed lignocellulose hydrolysis, though the content of xylan or mannan in lignocellulose after pretreatments is generally low. It is possible that the synergistic effect between cellulases and hemicellulases is partially due to the reduction of the cellulase trapping obstacles caused by hemicellulose and the creation of more highly reactive substrates.

It has been demonstrated that in cellulose hydrolysis the CD of the cellulase can be as effective as the intact enzyme that has both CD and CBM domains, provided that the substrate loading is high (10−20%).[47−49] The advantage of using the CD only is that the recycling of the CD is easier than that of the intact enzyme, especially in the presence of lignin, which binds irreversibly to CBM. Our results show that without CBM, the adsorption of Cel5A to PASC can be tuned by altering the amino acids in the binding surface of CD. Optimizing the binding property of cellulases may provide a new way to improve catalytic efficiency.

■ CONCLUSIONS

A *Tr.* Cel5A cellulose complex was modeled. Several important binding residues, including T18, K26, Y26, H229, and T300, were confirmed by the Cel5A PASC adsorption assays, whereas mutations of these residues and a few others from the binding fragments considerably perturb the adsorption affinity. The 19

dx.doi.org/10.1021/bi501059n | *Biochemistry* 2014, 53, 7650−7658

mutants tested experimentally have varied partitioning coefficients (K_r) ranging from 0.12 to 0.39 L/g, as compared to that of the WT (0.26 L/g). The kinetic measurements of the WT and mutants show that the hydrolysis power factor b is not correlated with the K_r but is anticorrelated with the activity A. This result indicates that the reaction slowdown is not correlated with the adsorption but is likely due to the decrease in substrate reactivity and enzyme trapping. The Cel5A PASC activity A is positively correlated with its specific activity against PNPC.

■ ASSOCIATED CONTENT

Supporting Information

One figure describing the Cel5A and cellulose complex model, one figure displaying the effect of cellobiose inhibition on Cel5A, two figures displaying the root-mean-square deviation of C_α atoms and the fluctuation of C_α atoms from MD trajectories, one figure fitting the WT Cel5A (0.25 μM) PASC hydrolysis kinetic data, one figure correlating c and K_r, two figures correlating the kinetic parameters from fitting to eqs 3 and 4, one figure displaying the concentration of free energy during PASC hydrolysis, one figure correlating the reaction rate with the PNPC concentration, two figures correlating the kinetic parameter b with binding parameters c and K_r, one figure displaying the fitting to eq 4, one figure correlating rate k_0 and PNPC specific activity, one figure displaying the fitting curve of WT Cel5A-catalyzed FP hydrolysis, one table of energies of interaction between Cel5A and cellulose, one table of hydrogen bonds formed between Cel5A and cellulose, one table of the amounts of sugar released from PASC hydrolysis, one table of kinetic parameters from fitting to eq 4, one table of kinetic parameters of WT Cel5A at different enzyme concentrations, one table of the amounts of reducing sugar released via FP hydrolysis, and one table of the amounts of soluble and total reducing sugars released. This material is available free of charge via the Internet at http://pubs.acs.org.

■ AUTHOR INFORMATION

Corresponding Author

*Room 413, QIBEBT, Qingdao 266061, China. E-mail: yaols@qibebt.ac.cn. Phone: 86 532 80662792. Fax: 86 532 80662778.

Funding

This work was supported in part by 100 Talent Project of the Chinese Academy of Sciences, the National Nature Science Foundation of China (Grants 21173247 and 31270785), the Foundation for Outstanding Young Scientist in Shandong Province (Grant JQ201104), and the "135" Projects Fund of the CAS-QIBEBT Director Innovation Foundation.

Notes

The authors declare no competing financial interest.

■ REFERENCES

(1) Yang, B., Willies, D. M., and Wyman, C. E. (2006) Changes in the Enzymatic Hydrolysis Rate of Avicel Cellulose with Conversion. *Biotechnol. Bioeng. 94*, 1122−1128.

(2) Bansal, P., Hall, M., Realff, M. J., Lee, J. H., and Bommarius, A. S. (2009) Modeling Cellulase Kinetics on Lignocellulosic Substrates. *Biotechnol. Adv. 27*, 833−848.

(3) Eriksson, T., Karlsson, J., and Tjerneld, F. (2002) A Model Explaining Declining Rate in Hydrolysis of Lignocellulose Substrates with Cellobiohydrolase I (Cel7A) and Endoglucanase I (Cel7B) of *Trichoderma reesei*. *Appl. Biochem. Biotechnol. 101*, 41−60.

(4) Gan, Q., Allen, S. J., and Taylor, G. (2003) Kinetic Dynamics in Heterogeneous Enzymatic Hydrolysis of Cellulose: An Overview, an Experimental Study and Mathematical Modelling. *Process Biochem. (Oxford, U.K.) 38*, 1003−1018.

(5) Zhang, S., Wolfgang, D. E., and Wilson, D. B. (1999) Substrate Heterogeneity Causes the Nonlinear Kinetics of Insoluble Cellulose Hydrolysis. *Biotechnol. Bioeng. 66*, 35−41.

(6) Hong, J., Ye, X. H., and Zhang, Y. H. P. (2007) Quantitative Determination of Cellulose Accessibility to Cellulase Based on Adsorption of a Nonhydrolytic Fusion Protein Containing CBM and GFP with Its Applications. *Langmuir 23*, 12535−12540.

(7) Divne, C., Stahlberg, J., Reinikainen, T., Ruohonen, L., Pettersson, G., Knowles, J. K. C., Teeri, T. T., and Jones, T. A. (1994) The 3-Dimensional Crystal Structure of the Catalytic Core of Cellobiohydrolase-I from *Trichoderma reesei*. *Science 265*, 524−528.

(8) Rouvinen, J., Bergfors, T., Teeri, T., Knowles, J. K. C., and Jones, T. A. (1990) 3-Dimensional Structure of Cellobiohydrolase-II from *Trichoderma reesei*. *Science 249*, 380−386.

(9) Kleywegt, G. J., Zou, J. Y., Divne, C., Davies, G. J., Sinning, I., Stahlberg, J., Reinikainen, T., Srisodsuk, M., Teeri, T. T., and Jones, T. A. (1997) The Crystal Structure of the Catalytic Core Domain of Endoglucanase I from *Trichoderma reesei* at 3.6 Angstrom Resolution, and a Comparison with Related Enzymes. *J. Mol. Biol. 272*, 383−397.

(10) Penttila, M., Lehtovaara, P., Nevalainen, H., Bhikhabhai, R., and Knowles, J. (1986) Homology between Cellulase Genes of *Trichoderma reesei* Complete Nucleotide Sequence of the Endoglucanase-I Gene. *Gene 45*, 253−263.

(11) Lee, T. M., Farrow, M. F., Arnold, F. H., and Mayo, S. L. (2011) A Structural Study of *Hypocrea jecorina* Cel5A. *Protein Sci. 20*, 1935−1940.

(12) Saloheimo, M., Lehtovaara, P., Penttila, M., Teeri, T. T., Stahlberg, J., Johansson, G., Pettersson, G., Claeyssens, M., Tomme, P., and Knowles, J. K. C. (1988) Egiii, a New Endoglucanase from *Trichoderma reesei*: The Characterization of Both Gene and Enzyme. *Gene 63*, 11−21.

(13) Sandgren, M., Shaw, A., Ropp, T. H., Bott, S. W. R., Cameron, A. D., Stahlberg, J., Mitchinson, C., and Jones, T. A. (2001) The X-ray Crystal Structure of the *Trichoderma reesei* Family 12 Endoglucanase 3, Cel12A, at 1.9 Angstrom Resolution. *J. Mol. Biol. 308*, 295−310.

(14) Murphy, L., Cruys-Bagger, N., Damgaard, H. D., Baumann, M. J., Olsen, S. N., Borch, K., Lassen, S. F., Sweeney, M., Tatsumi, H., and Westh, P. (2012) Origin of Initial Burst in Activity for *Trichoderma reesei* Endo-Glucanases Hydrolyzing Insoluble Cellulose. *J. Biol. Chem. 287*, 1252−1260.

(15) Cruys-Bagger, N., Elmerdahl, J., Praestgaard, E., Tatsumi, H., Spodsberg, N., Borch, K., and Westh, P. (2012) Pre-Steady-State Kinetics for Hydrolysis of Insoluble Cellulose by Cellobiohydrolase Cel7A. *J. Biol. Chem. 287*, 18451−18458.

(16) Murphy, L., Bohlin, C., Baumann, M. J., Olsen, S. N., Sorensen, T. H., Anderson, L., Borch, K., and Westh, P. (2013) Product Inhibition of Five *Hypocrea jecorina* Cellulases. *Enzyme Microb. Technol. 52*, 163−169.

(17) Jalak, J., and Valjamae, P. (2010) Mechanism of Initial Rapid Rate Retardation in Cellobiohydrolase Catalyzed Cellulose Hydrolysis. *Biotechnol. Bioeng. 106*, 871−883.

(18) Kurasin, M., and Valjamae, P. (2011) Processivity of Cellobiohydrolases Is Limited by the Substrate. *J. Biol. Chem. 286*, 169−177.

(19) Cruys-Bagger, N., Tatsumi, H., Ren, G. R., Borch, K., and Westh, P. (2013) Transient Kinetics and Rate-Limiting Steps for the Processive Cellobiohydrolase Cel7A: Effects of Substrate Structure and Carbohydrate Binding Domain. *Biochemistry 52*, 8938−8948.

(20) Suominen, P. L., Mantyla, A. L., Karhunen, T., Hakola, S., and Nevalainen, H. (1993) High-Frequency One-Step Gene Replacement in *Trichoderma reesei*. 2. Effects of Deletions of Individual Cellulase Genes. *Mol. Gen. Genet. 241*, 523−530.

(21) Claeyssens, M., and Henrissat, B. (1992) Specificity Mapping of Cellulolytic Enzymes: Classification into Famillies of Structurally

Related Proteins Confirmed by Biochemical Analysis. *Protein Sci. 1*, 1293−1297.
(22) Nakazawa, H., Okada, K., Kobayashi, R., Kubota, T., Onodera, T., Ochiai, N., Omata, N., Ogasawara, W., Okada, H., and Morikawa, Y. (2008) Characterization of the Catalytic Domains of *Trichoderma reesei* Endoglucanase I, II, and III, Expressed in *Escherichia coli*. *Appl. Microbiol. Biotechnol. 81*, 681−689.
(23) Olsson, M. H. M., Sondergaard, C. R., Rostkowski, M., and Jensen, J. H. (2011) PROPKA3: Consistent Treatment of Internal and Surface Residues in Empirical pK_a Predictions. *J. Chem. Theory Comput. 7*, 525−537.
(24) Nishiyama, Y., Langan, P., and Chanzy, H. (2002) Crystal Structure and Hydrogen-Bonding System in Cellulose Iβ from Synchrotron X-ray and Neutron Fiber Diffraction. *J. Am. Chem. Soc. 124*, 9074−9082.
(25) Ghoorah, A. W., Devignes, M. D., Smail-Tabbone, M., and Ritchie, D. W. (2013) Protein Docking Using Case-Based Reasoning. *Proteins 81*, 2150−2158.
(26) Hess, B., Kutzner, C., van der Spoel, D., and Lindahl, E. (2008) GROMACS 4: Algorithms for Highly Efficient, Load-Balanced, and Scalable Molecular Simulation. *J. Chem. Theory Comput. 4*, 435−447.
(27) Van der Spoel, D., Lindahl, E., Hess, B., Groenhof, G., Mark, A. E., and Berendsen, H. J. C. (2005) GROMACS: Fast, Flexible, and Free. *J. Comput. Chem. 26*, 1701−1718.
(28) Pol-Fachin, L., Rusu, V. H., Verli, H., and Lins, R. D. (2012) GROMOS 53A6(GLYC), an Improved GROMOS Force Field for Hexopyranose-Based Carbohydrates. *J. Chem. Theory Comput. 8*, 4681−4690.
(29) Oostenbrink, C., Villa, A., Mark, A. E., and Van Gunsteren, W. F. (2004) A Biomolecular Force Field Based on the Free Enthalpy of Hydration and Solvation: The GROMOS Force-Field Parameter Sets 53A5 and 53A6. *J. Comput. Chem. 25*, 1656−1676.
(30) Zhang, Y.-H. p., Cui, J., Lynd, L. R., and Kuang, L. R. (2006) A Transition from Cellulose Swelling to Cellulose Dissolution by Phosphoric Acid: Evidence from Enzymatic Hydrolysis and Supramolecular Structure. *Biomacromolecules 7*, 644−648.
(31) Lever, M. (1972) New Reaction for Colorimetric Determination of Carbohydrates. *Anal. Biochem. 47*, 273−279.
(32) Gilkes, N. R., Jervis, E., Henrissat, B., Tekant, B., Miller, R. C., Warren, R. A. J., and Kilburn, D. G. (1992) The Adsorption of a Bacterial Cellulase and Its 2 Isolated Domains to Crystalline Cellulose. *J. Biol. Chem. 267*, 6743−6749.
(33) Kostylev, M., and Wilson, D. (2013) Two-Parameter Kinetic Model Based on a Time-Dependent Activity Coefficient Accurately Describes Enzymatic Cellulose Digestion. *Biochemistry 52*, 5656−5664.
(34) Kostylev, M., Alahuhta, M., Chen, M., Brunecky, R., Himmel, M. E., Lunin, V. V., Brady, J., and Wilson, D. B. (2014) Cel48A From *Thermobifida fusca*: Structure and Site Directed Mutagenesis of Key Residues. *Biotechnol. Bioeng. 111*, 664−673.
(35) Lee, T. M., Farrow, M. F., Arnold, F. H., and Mayo, S. L. (2011) A Structural Study of *Hypocrea jecorina* Cel5A. *Protein Sci. 20*, 1935−1940.
(36) Ohmine, K., Ooshima, H., and Harano, Y. (1983) Kinetic-Study on Enzymatic-Hydrolysis of Cellulose by Cellulase from *Trichoderma viride*. *Biotechnol. Bioeng. 25*, 2041−2053.
(37) Nidetzky, B., Zachariae, W., Gercken, G., Hayn, M., and Steiner, W. (1994) Hydrolysis of Cellooligosaccharides by *Trichoderma reesei* Cellobiohydrolases: Experimental Data and Kinetic Modeling. *Enzyme Microb. Technol. 16*, 43−52.
(38) Horn, S. J., Sikorski, P., Cederkvist, J. B., Vaaje-Kolstad, G., Sorlie, M., Synstad, B., Vriend, G., Varum, K. M., and Eijsink, V. G. H. (2006) Costs and Benefits of Processivity in Enzymatic Degradation of Recalcitrant Polysaccharides. *Proc. Natl. Acad. Sci. U.S.A. 103*, 18089−18094.
(39) Uchiyama, T., Katouno, F., Nikaidou, N., Nonaka, T., Sugiyama, J., and Watanabe, T. (2001) Roles of the Exposed Aromatic Residues in Crystalline Chitin Hydrolysis by Chitinase A from *Serratia marcescens 2170*. *J. Biol. Chem. 276*, 41343−41349.
(40) Zakariassen, H., Eijsink, V. G. H., and Sorlie, M. (2010) Signatures of Activation Parameters Reveal Substrate-Dependent Rate Determining Steps in Polysaccharide Turnover by a Family 18 Chitinase. *Carbohydr. Polym. 81*, 14−20.
(41) Zakariassen, H., Aam, B. B., Horn, S. J., Varum, K. M., Sorlie, M., and Eijsink, V. G. H. (2009) Aromatic Residues in the Catalytic Center of Chitinase A from *Serratia marcescens* Affect Processivity, Enzyme Activity, and Biomass Converting Efficiency. *J. Biol. Chem. 284*, 10610−10617.
(42) Phillips, C. M., Beeson, W. T., Cate, J. H., and Marletta, M. A. (2011) Cellobiose Dehydrogenase and a Copper-Dependent Polysaccharide Monooxygenase Potentiate Cellulose Degradation by *Neurospora crassa*. *ACS Chem. Biol. 6*, 1399−1406.
(43) Langston, J. A., Shaghasi, T., Abbate, E., Xu, F., Vlasenko, E., and Sweeney, M. D. (2011) Oxidoreductive Cellulose Depolymerization by the Enzymes Cellobiose Dehydrogenase and Glycoside Hydrolase 61. *Appl. Environ. Microbiol. 77*, 7007−7015.
(44) Penttila, P. A., Varnai, A., Pere, J., Tammelin, T., Salmen, L., Siika-aho, M., Viikari, L., and Serimaa, R. (2013) Xylan as a Limiting Factor in Enzymatic Hydrolysis of Nanocellulose. *Bioresour. Technol. 129*, 135−141.
(45) Billard, H., Faraj, A., Lopes Ferreira, N., Menir, S., and Heiss-Blanquet, S. (2012) Optimization of a Synthetic Mixture Composed of Major *Trichoderma reesei* Enzymes for the Hydrolysis of Steam-Exploded Wheat Straw. *Biotechnol. Biofuels 5*, 9.
(46) Varnai, A., Huikko, L., Pere, J., Siika-aho, M., and Viikari, L. (2011) Synergistic Action of Xylanase and Mannanase Improves the Total Hydrolysis of Softwood. *Bioresour. Technol. 102*, 9096−9104.
(47) Pakarinen, A., Haven, M. O., Djajadi, D. T., Varnai, A., Puranen, T., and Viikari, L. (2014) Cellulases without Carbohydrate-Binding Modules in High Consistency Ethanol Production Process. *Biotechnol. Biofuels 7*, 27.
(48) Varnai, A., Siika-aho, M., and Viikari, L. (2013) Carbohydrate-Binding Modules (CBMs) Revisited: Reduced Amount of Water Counterbalances the Need for CBMs. *Biotechnol. Biofuels 6*, 30.
(49) Le Costaouec, T., Pakarinen, A., Varnai, A., Puranen, T., and Viikari, L. (2013) The Role of Carbohydrate Binding Module (CBM) at High Substrate Consistency: Comparison of *Trichoderma reesei* and *Thermoascus aurantiacus* Cel7A (CBHI) and Cel5A (EGII). *Bioresour. Technol. 143*, 196−203.